Electronic Supplementary Material (ESI) for RSC Sustainability.

Supporting Document

Platinum-Tin as a Superior Catalyst for Proton Exchange Membrane Fuel Cells

Prabal Sapkota[1], Sean Lim [2], Kondo-Francois Aguey-Zinsou*[3]

[1]MERLin, School of Chemical Engineering, The University of New South Wales, Sydney, NSW 2052, Australia

[2]Electron Microscope Unit, University of New South Wales, Sydney, NSW 2052, Australia

[3]MERLin, School of Chemistry, University of Sydney, NSW 2006, Australia,

*E-mail: f.aguey@sydney.edu.au

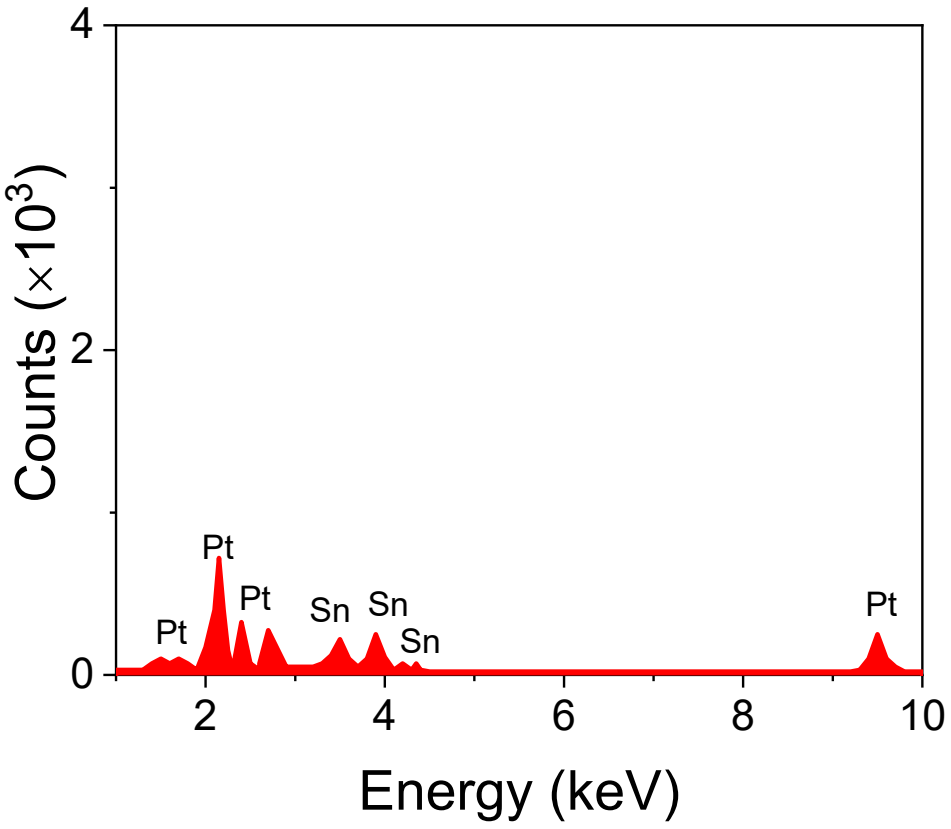

Fig. S1 EDX plot of PtSn/VC(3).

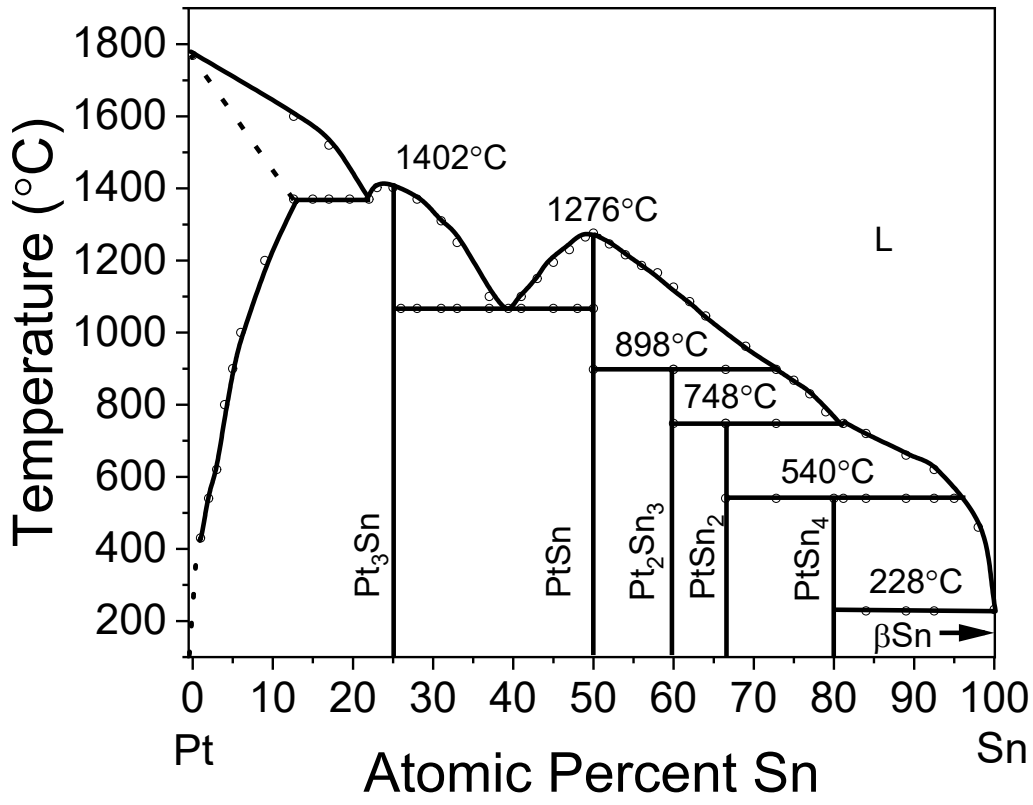

Fig. S2 Pt-Sn Phase diagram.[1]

The Pt-Sn phase diagram is shown in Fig. S2. The as-synthesized catalysts with various ratios of Pt to Sn are in-line with the phase diagram, in particular, PtSn was obtained with 60wt% of Pt and 40wt% of Sn. Pt_2Sn_3 was obtained with 52wt% of Pt and 48wt% of Sn.

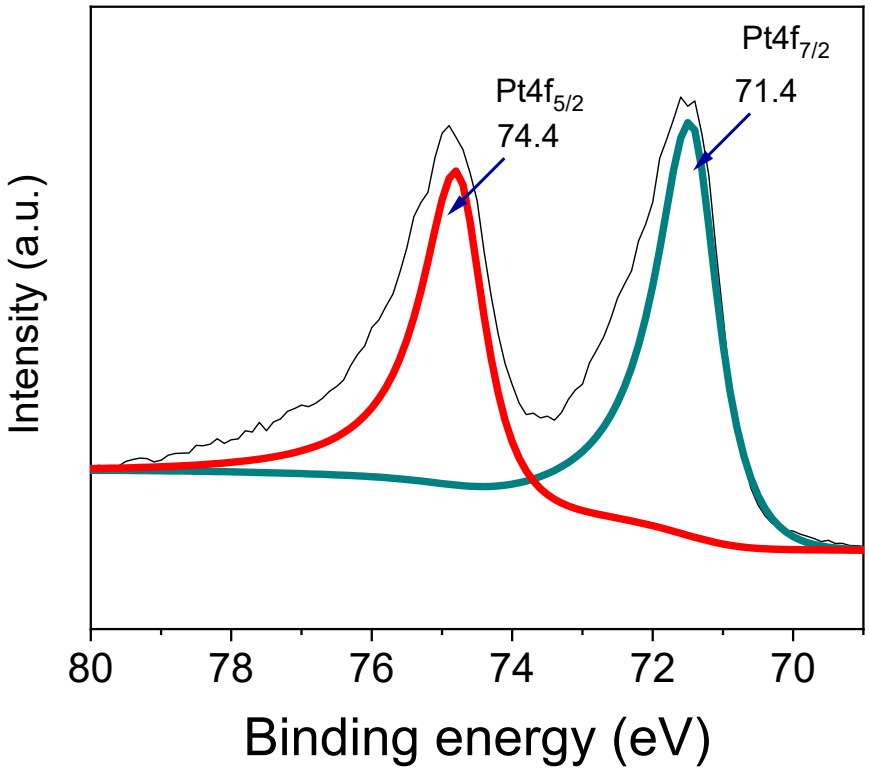

Fig. S3 XPS spectra of as-synthesized Pt/VC.

The XPS of as-synthesized Pt is shown in Fig. S3. The binding energies of Pt4f at 74.4 and 71.4 eV are assigned to Pt.

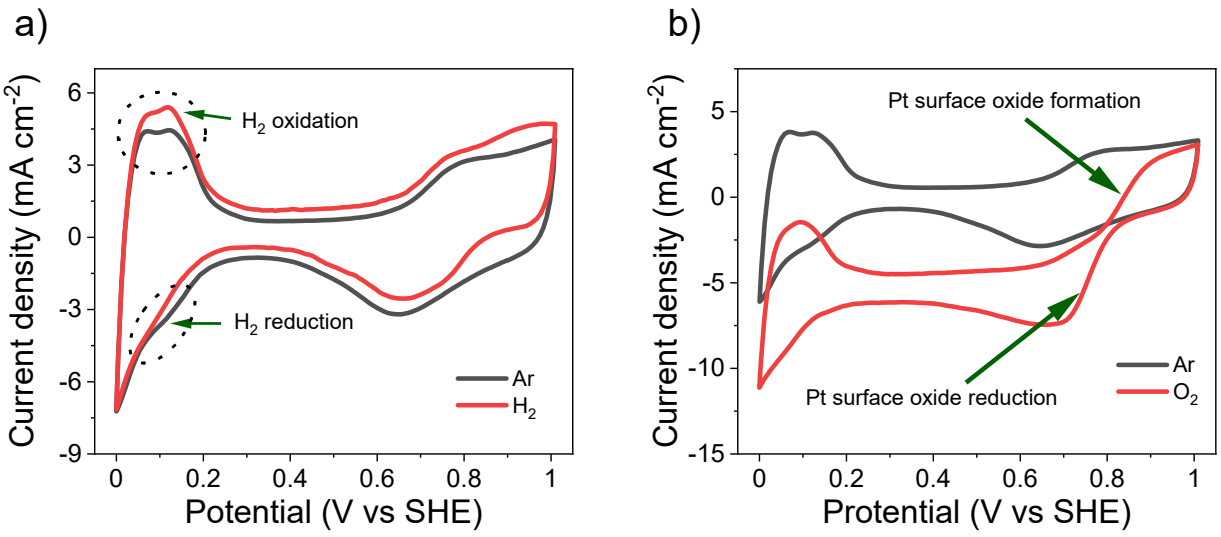

Fig. S4 CV of as-synthesized Pt/VC at scan rate 50 mV s^{-1} @ 1600 rpm in 0.1M aqueous $HClO_4$ under saturated Ar and O_2, (a) under saturated Ar and H_2, (b) under saturated Ar and O_2. Catalyst loading was 50 µg cm^{-2}.

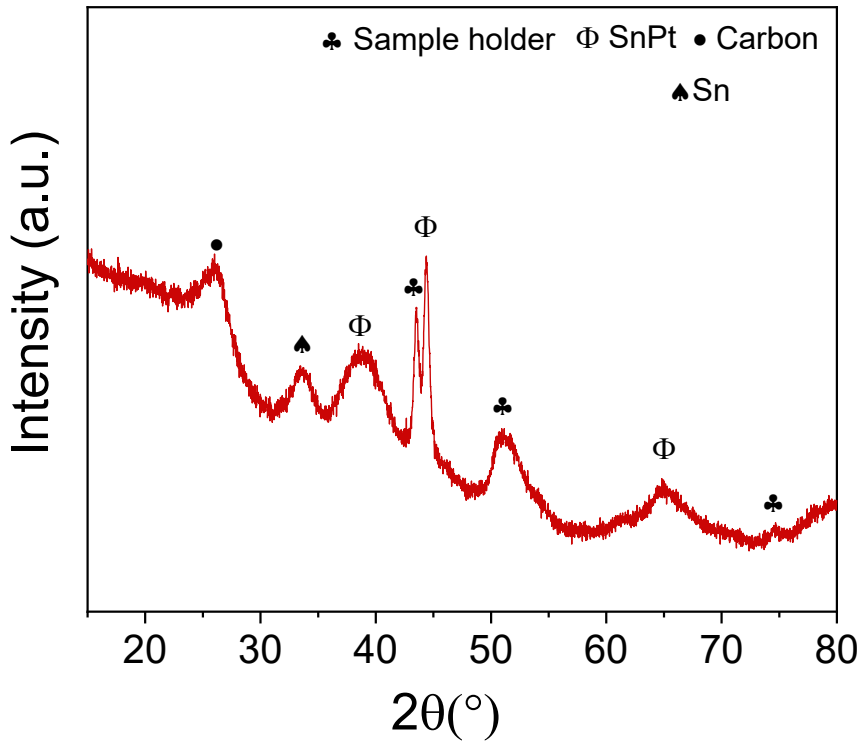

Fig. S5 XRD pattern of as-synthesized PtSn/VC(1.5).

The XRD pattern of as-synthesized Pt/Sn(1.5) is shown in Fig. S5. The diffraction peaks at 38.9, 44.4 and 65.1° are assigned to cubic PtSn(111), PtSn(200) and PtSn(220), respectively. A small diffraction peak related to Sn was observed at 33.3° in all the alloys.[2]

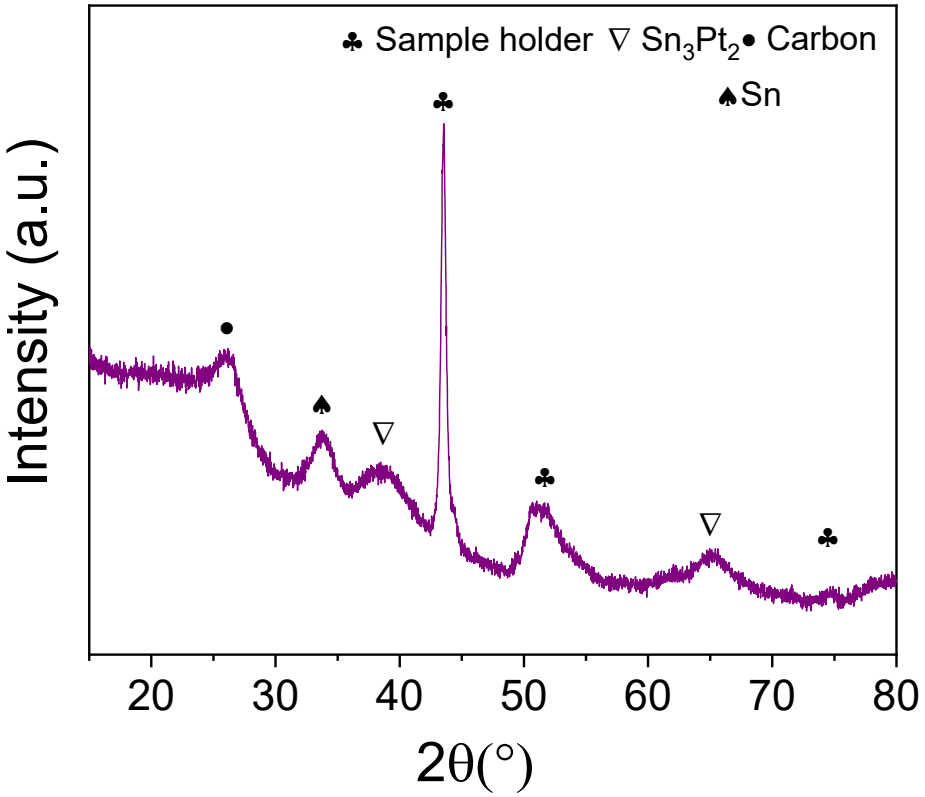

Fig. S6 XRD pattern of as-synthesized PtSn/VC(1.0).

The XRD pattern of as-synthesized Pt/Sn(1.0) is shown in Fig. S6. The diffraction peaks at 38.7 and 65.2° are assigned to cubic Sn_3Pt_2(111) and Sn_3Pt_2(220), respectively. A small diffraction peak related to Sn was observed at 33.3° in all the alloys.[2]

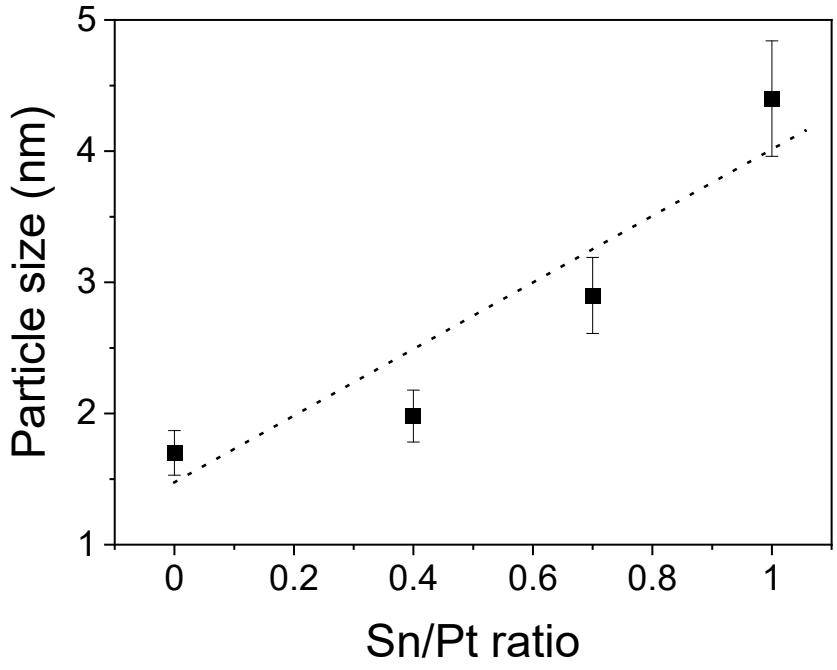

Fig. S7 Comparison of particle size of the as-synthesized catalysts as function of the Sn/Pt ratio. This was calculated by using the Scherrer equation.[3]

Characterization of commercial 40%Pt/VC (noted as Pt*/VC)

The TEM image of Pt*/VC is shown Fig. S8. TEM revealed Pt particles with an average size of 2.5 nm dispersed on Vulcan carbon (Fig. S8d). The XRD of Pt*/VC is shown Fig. S10.

The electrocatalytic activity of Pt*/VC was determined by the RDE method. Fig. S11a shows the CV profile obtained in 0.1M aqueous $HClO_4$ under saturated Ar and H_2 at the scan rate of 50 mV s^{-1}. Under Ar, the cathodic and anodic CV features between 0.05 and 0.2 V correspond to the adsorption and desorption of underpotential deposited H (H_{UPD}), respectively.[4] Similarly, the anodic feature in between 0.6 and 1.0 V corresponds to the formation of Pt surface oxides. The cathodic feature between 0.5 and 1.0 V is due to the reduction of the oxide layer at the Pt surface. Under saturated H_2, a higher current was observed on the CV profile due to the occurring HOR and this was related to the typical features associated with the adsorption and desorption of H_{UPD} at the Pt surface.

ORR activity was also analyzed. Fig. S12a shows the CV under saturated Ar and O_2 at the scan rate of 50 mV s^{-1}. As in the case of HOR, under saturated Ar, the cathodic and anodic CV profile in between 0.05 and 0.2 V are assigned to adsorption and desorption of H_{UPD}, respectively. Similarly, the anodic features in between 0.6 and 1.0 V correspond to the formation of Pt surface oxides, and the cathodic feature in the voltage range 0.5 - 1.0 V is due to the reduction of these surface oxides. Under saturated O_2, in addition to the typical features associated with the underlying adsorption and desorption of $H_{UPD,}$ larger currents due to the reduction and oxidation of dissolved O_2 at the Pt surface are observed.

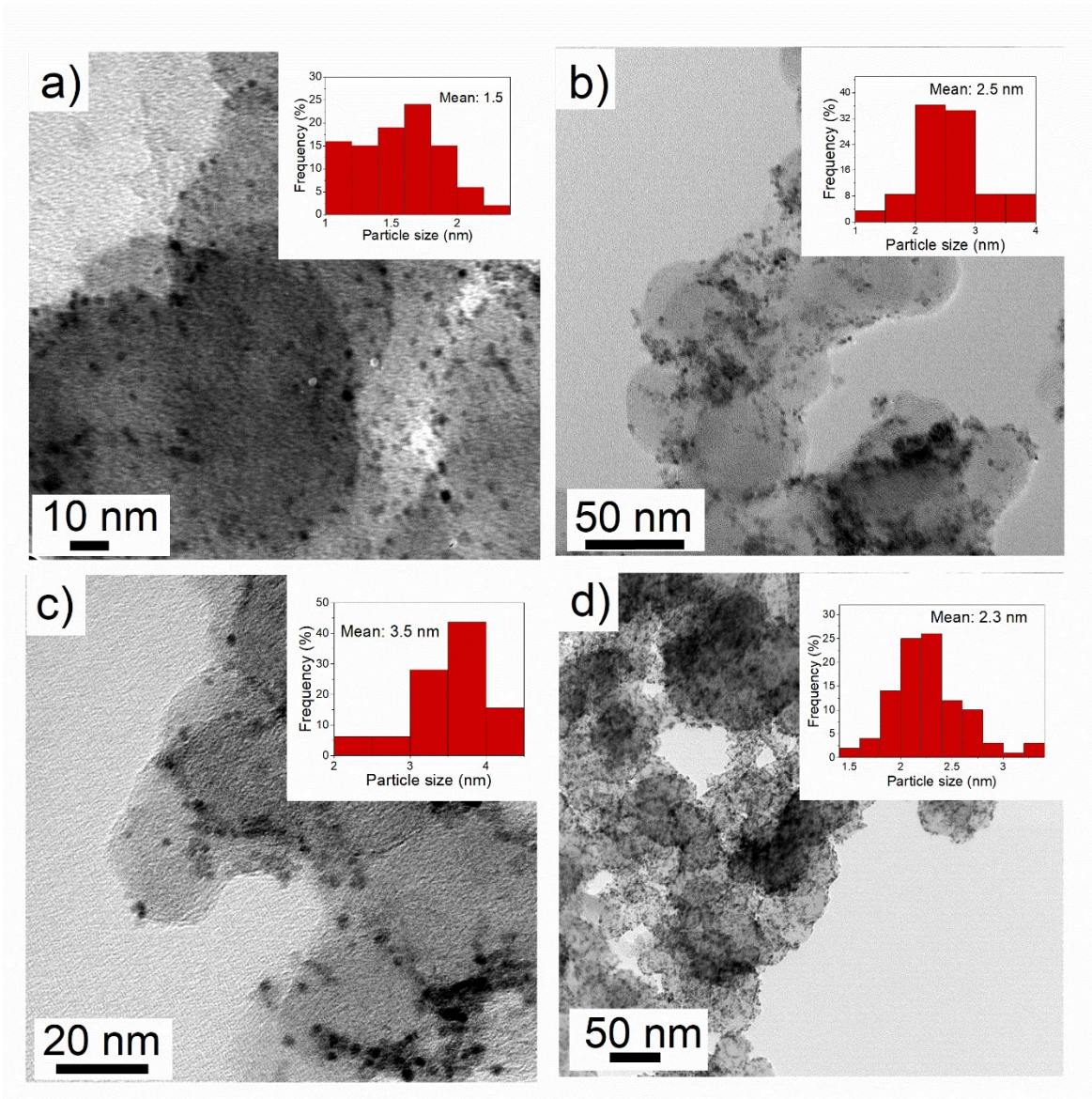

Fig. S8 TEM images of a) Pt/VC, b) PtSn/VC(1.5) c) PtSn/VC(1.0), and d) commercial 40%Pt/VC (noted as Pt*/VC). Particles with average size of 1.5 ± 0.30 nm, 2.5 ± 0.50 nm, 3.5 ± 0.52 nm and 2.3 ± 0.35 nm were observed for Pt/VC, PtSn/VC(1.5), PtSn/VC(1) and Pt*/VC, respectively.

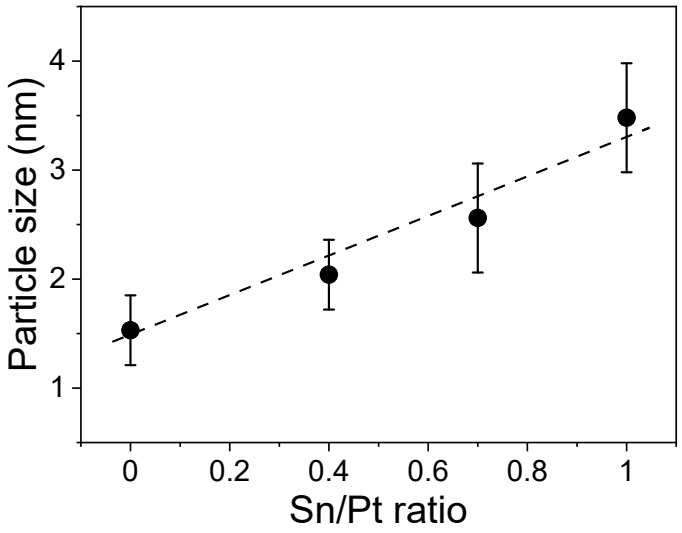

Fig. S9 Comparison of particle size as determined by TEM analysis of the as-synthesized catalysts as function of the Sn/Pt ratio.

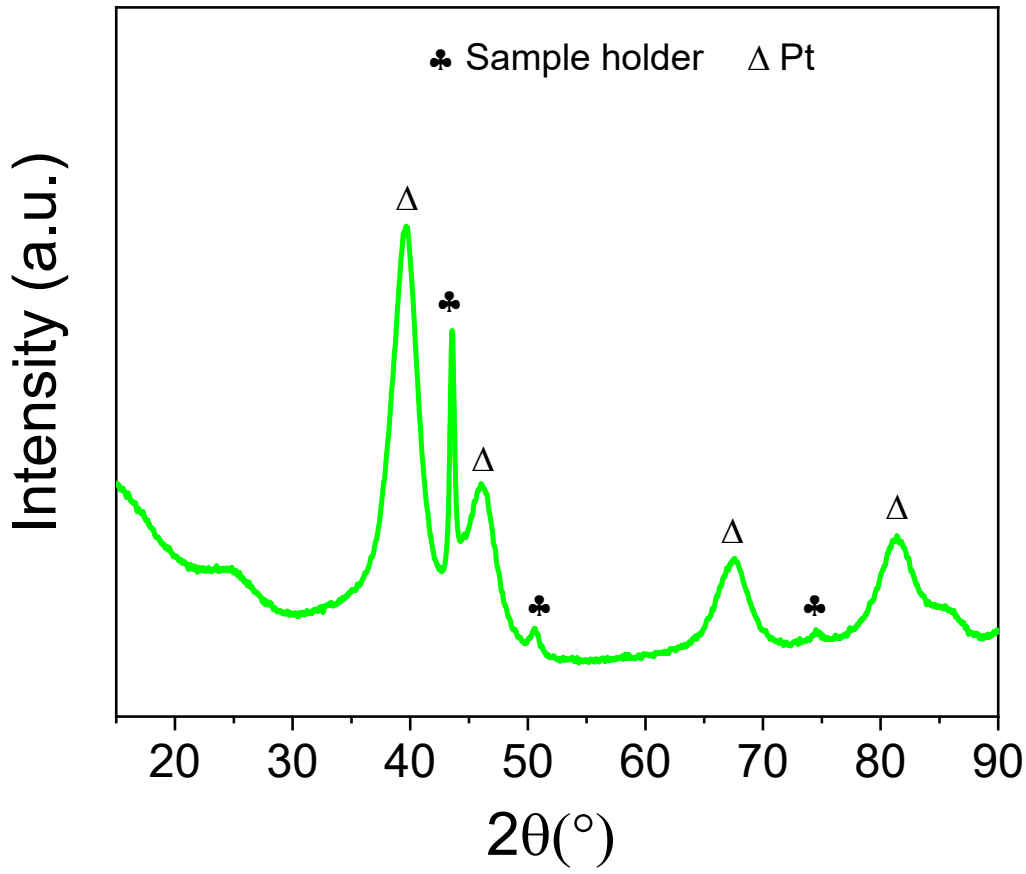

Fig. S10 XRD pattern of Pt*/VC.

The XRD pattern of Pt*/VC is shown in Fig. S10. The diffraction peaks at 39.6, 46.2, 67.7 and 81.5° were assigned to Pt(111), Pt(200), Pt(220) and Pt(311), respectively.

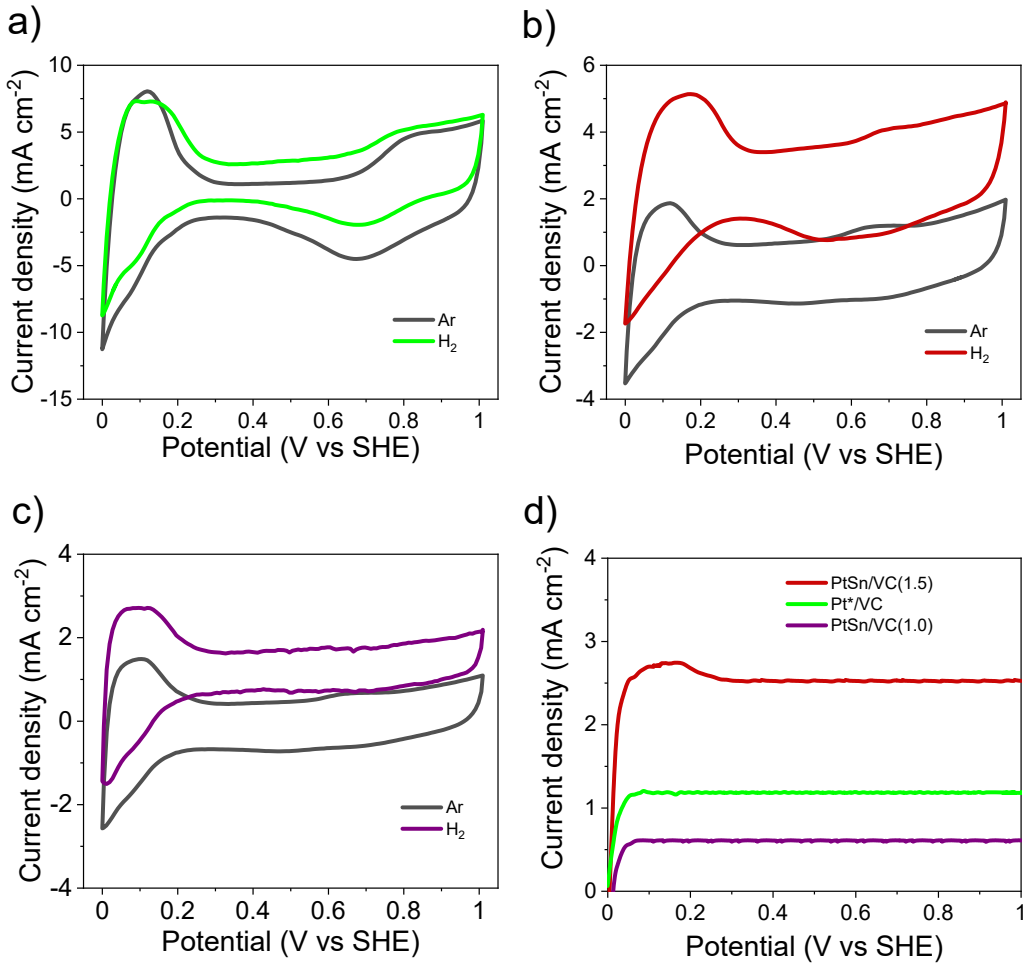

Fig. S11 HOR activity CV @ 50 mV s^{-1} of: (a) Pt*/VC, (b) PtSn/VC(1.5), (c) PtSn/VC(1.0), (d) LSV at a scan rate of 10 mVs^{-1} @ 1600 rpm. The catalyst loading was 50 µg cm^{-2}.

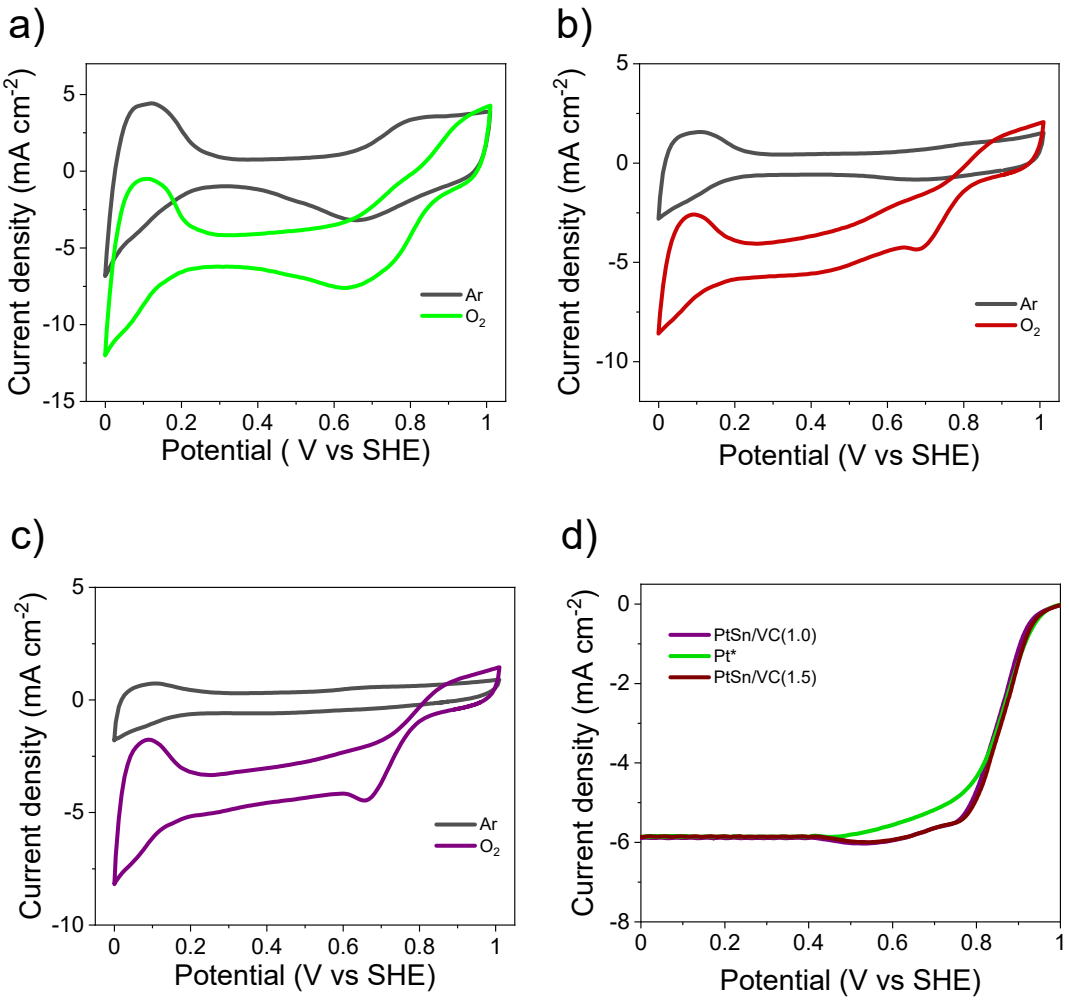

Fig. S12 ORR activity CV @ 50 mV s^{-1} of: (a) Pt*/VC, (b) PtSn/VC(1.5), c) PtSn/VC(1.0), (d) LSV at a scan rate of 10 mVs^{-1} @ 1600 rpm. The catalyst loading was 50 µg cm^{-2}.

Electrochemical surface area (ECSA) and mass activity (MA) calculation

The procedure to calculate ECSA and MA has been discussed in the literature.[5-7] In brief,

$$ECSA\ (m^2 g_{Pt}^{-1}) = \left(\frac{Q_{H-adsorption}(C)}{210\mu C\ cm_{Pt}^{-2} L_{Pt}\left(mg_{Pt} cm^{-2}\right) A_g cm^2}\right) 10^5$$

where, $Q_{H-adsorption}$ is the charge obtained from the integrated area of hydrogen adsorption in the region 0.03 - 0.3V of CV, L_{Pt} is the working electrode Pt loading and A_g is the geometric surface area of the glassy carbon electrode, $210\ \mu C$ is the conversion factor (charge density of bulk polycrystalline Pt).

Similarly,

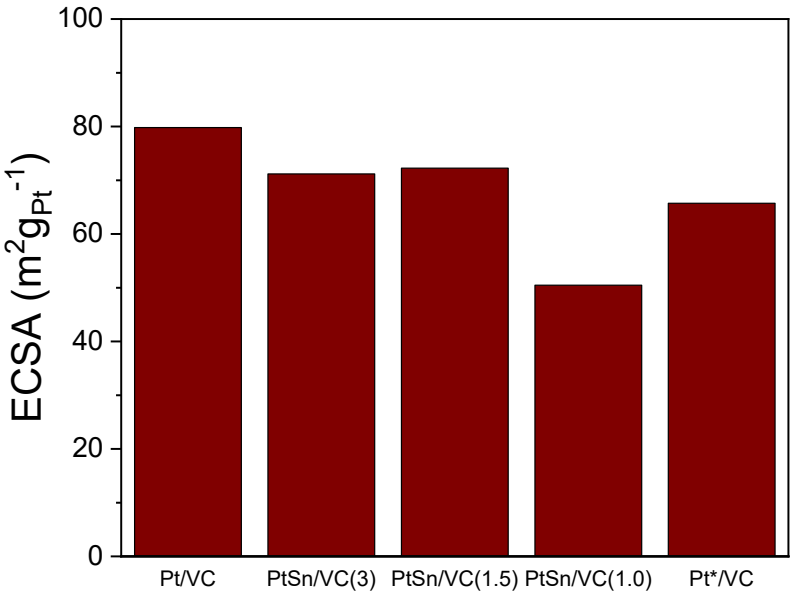

Fig. S13 Electrochemical surface area (ESCA) of the catalysts.

The mass activity of the catalyst was calculated by using the expression (2).[5-7]

$$Mass\ activity = \frac{j_k}{m_{Pt}} \qquad (2)$$

where m_{Pt} is the Pt loading on the glassy carbon, j_k is the kinetic current density calculated from the Koutecky - levich equation (3).

$$\frac{1}{j_k} = \frac{1}{j} - \frac{1}{j_d} \qquad (3)$$

where, j is Faradic current density and j_d is the diffusion current density.

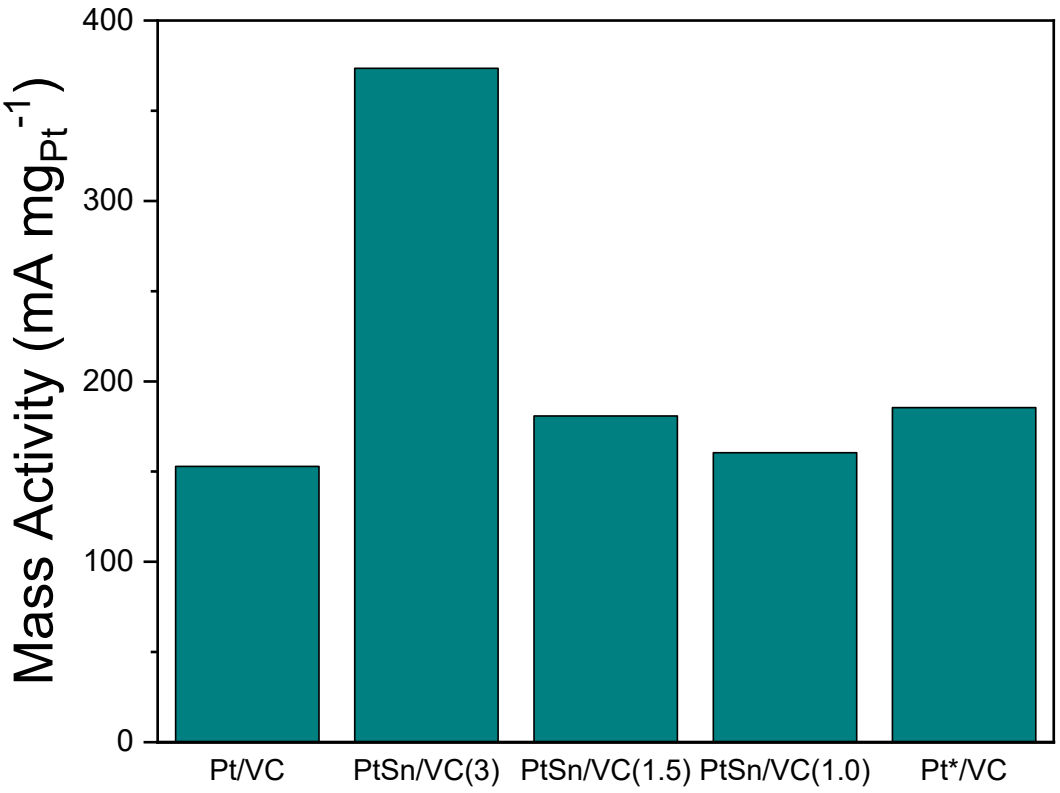

Fig. S14 Mass activity of the catalysts at 0.9 V.

Calculations of number of electrons transferred

The Koutecky-Levich analysis was used to calculate the number of electrons transferred during ORR. For this, I^{-1} vs $\omega^{-1/2}$ was plotted as shown Fig. S15, where I is the current density (A cm^{-2}) at the rotating disk electrode, and ω is the rotation rate of the rotating disk electrode. The number of electrons exchanged per O_2 molecule reacted was calculated from the inverse of the slopes (eq. 1) of the I^{-1} vs $\omega^{-1/2}$ plots (Fig. S15).

$$(Slope)^{-1} = 0.2nFAD^{2/3}v^{-1/6}C \qquad (1)$$

where, n is the number of electrons transferred, F is the Faraday constant (96487 C mol^{-1}), A is the electrode area, D is the diffusion coefficient of O_2 (1.9×10^{-5} cm^2 s^{-1}), υ is the kinematic viscosity of water (0.01 cm^2 s^{-1}), C is the concentration of O_2 solution (1.1×10^{-5} mol cm^{-3}).[8, 9] The number of electrons transferred during ORR is shown in Fig. S16.

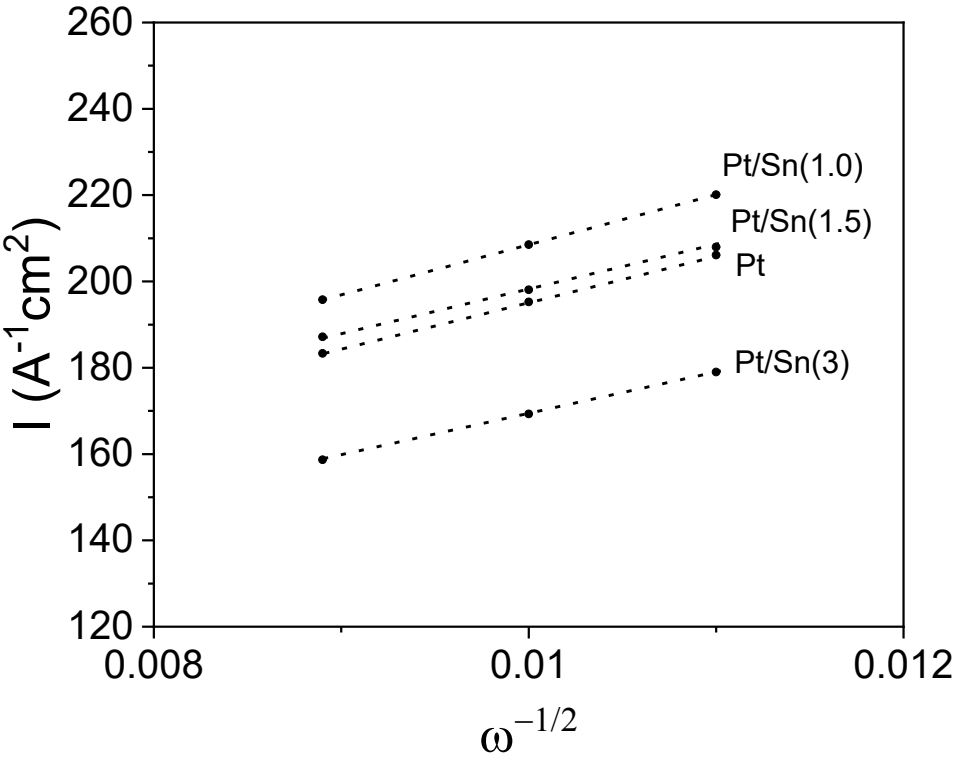

Fig. S15 Koutecky–Levich plots for the various catalysts at 0.6 V vs. SHE.

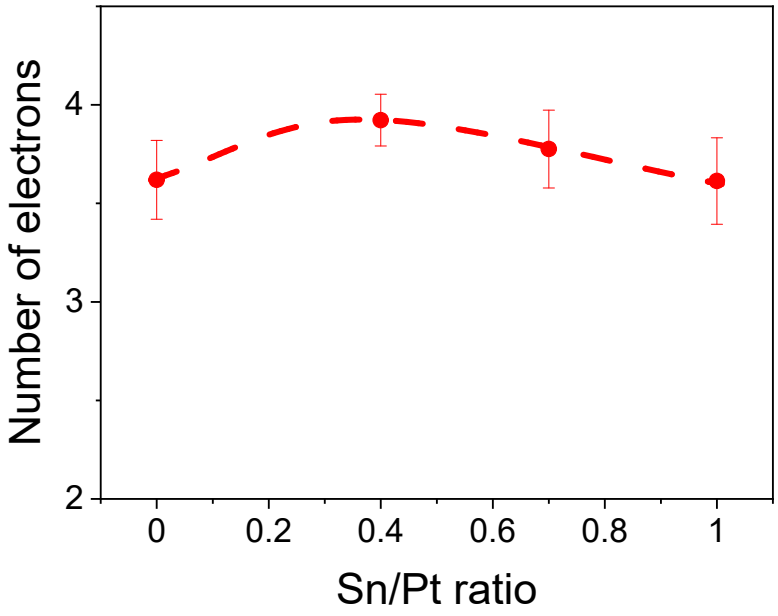

Fig. S16 Number of electrons transferred during ORR at various Sn/Pt ratios. The calculation was derived from the Koutecky-Levich analysis Fig. S15.

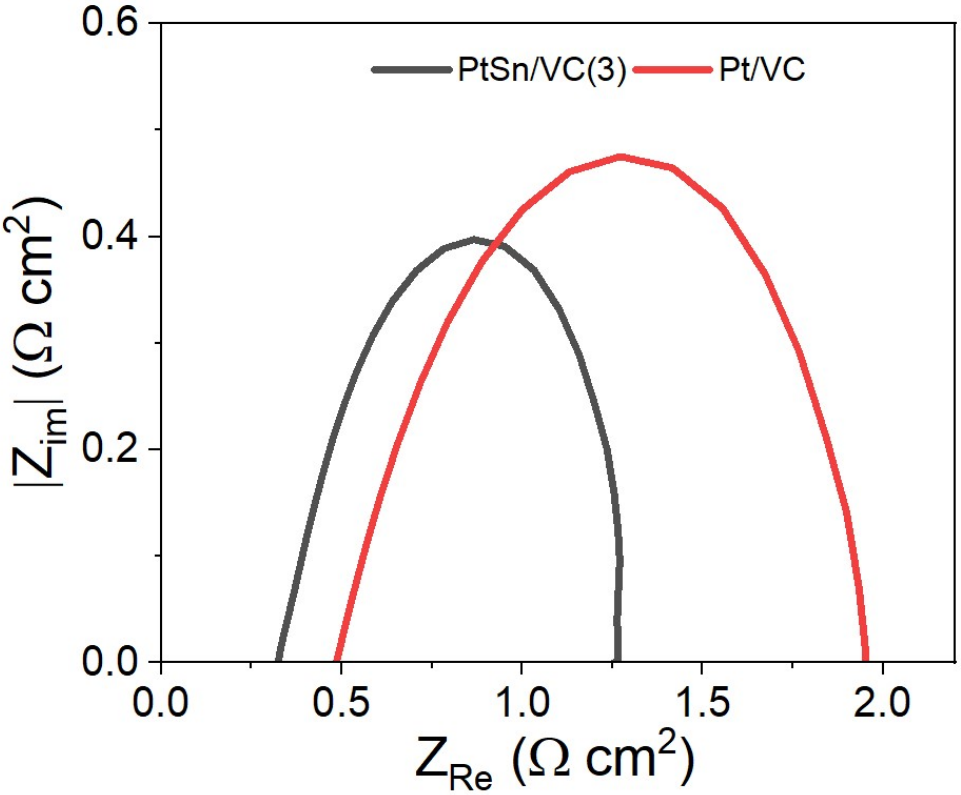

Fig. S17 EIS of PtSn/VC(3) and Pt/VC under self-breathing PEMFC operation at 25 °C and H_2 humidified at 20% RH at the anode. A current response was monitored at 0.5 V vs the standard hydrogen electrode by applying a sinusoidal input with an amplitude of 30 mV. The selected frequency was between 100 kHz and 0.1 Hz from high to low frequency.

The first intercept observed on the Electrochemical Impedance Spectroscopy (EIS) curve on x-axis is the ohmic resistance (R_{ohm}) and the length between the first and the second intercept of the curve on the x-axis corresponds to charge transfer resistance (R_{ct}).[10] As shown in Fig. S17, R_{ohm} with Pt/VC ~ 0.49 Ω cm^2 was higher than that of PtSn/VC(3), ~0.39 Ω cm^2. Higher value of R_{ct} was also observed with Pt/VC in comparison to PtSn/VC(3), 1.95 Ωcm^2 and 1.26 Ωcm^2

respectively for Pt/VC and PtSn/VC(3). This shows that the activity of PtSn/VC(3) catalyst is higher than Pt/VC under self-breathing PEMFC operation.

References

1. H. Okamoto, *Journal of Phase Equilibria*, 2003, **24**, 276-276.
2. E. Antolini, *International Journal of Hydrogen Energy*, 2011, **36**, 11043-11047.
3. H. Y. Hsu and B. J. Tongol, *Advances in Natural Sciences: Nanoscience and Nanotechnology*, 2013, **4**.
4. S. Tahmasebi, A. A. McMath, J. van Drunen and G. Jerkiewicz, *Electrocatalysis*, 2017, **8**, 301-310.
5. Y. Garsany, O. A. Baturina, K. E. Swider-Lyons and S. S. Kocha, *Analytical Chemistry*, 2010, **82**, 6321-6328.
6. Y. F. Xia, P. Guo, J. Z. Li, L. Zhao, X. L. Sui, Y. Wang and Z. B. Wang, *iScience*, 2021, **24**, 103024.
7. K. J. J. Mayrhofer, D. Strmcnik, B. B. Blizanac, V. Stamenkovic, M. Arenz and N. M. Markovic, *Electrochimica Acta*, 2008, **53**, 3181-3188.
8. J. Wu and H. Yang, *Nano Research*, 2010, **4**, 72-82.
9. C. Paliteiro and N. Martins, *Electrochimica Acta*, 1998, **44**, 1359-1368.
10. P. Sapkota, P. Brockbank and K.-F. Aguey-Zinsou, *International Journal of Hydrogen Energy*, 2022, **47**, 23833-23844.